

Available online at [www.sciencedirect.com](http://www.sciencedirect.com)

ScienceDirect

journal homepage: <http://Elsevier.com/locate/radcr>

## Case Report

# Radiologic presentation of chronic granulomatous prostatitis mimicking locally advanced prostate adenocarcinoma

Su-Min Lee <sup>a,\*</sup>, Jay Joshi <sup>b</sup>, Konrad Wolfe <sup>c</sup>, Peter Acher <sup>a</sup>, Sidath H. Liyanage <sup>b</sup>

<sup>a</sup> Department of Urology, Southend University Hospital, Prittlewell Chase, Westcliff-on-Sea, Essex, SSO 0RY, UK

<sup>b</sup> Department of Radiology, Southend University Hospital, Prittlewell Chase, Westcliff-on-Sea, Essex, SSO 0RY, UK

<sup>c</sup> Department of Pathology, Southend University Hospital, Prittlewell Chase, Westcliff-on-Sea, Essex, SSO 0RY, UK

## ARTICLE INFO

## Article history:

Received 26 December 2015

Accepted 8 February 2016

Available online 16 March 2016

## Keywords:

Granulomatous prostatitis

Prostate

MRI

## ABSTRACT

We present a case of nonspecific granulomatous prostatitis (GP), a clinical mimic of prostate adenocarcinoma. A 54-year-old man presented with lower urinary tract symptoms and raised prostate-specific antigen. Magnetic resonance imaging showed features consistent with prostate cancer, including low T2-signal intensity in the peripheral and transition zones with signs of extracapsular extension. Diffusion-weighted imaging showed high-signal intensity, with low apparent diffusion coefficient values, whereas dynamic contrast enhancement demonstrated a type 3 washout curve, similar to that found in prostate cancer. Transperineal sector-guided prostate biopsy confirmed nonspecific GP, and the patient was treated conservatively. We discuss and compare nonspecific, chronic GP as a radiologic mimic of prostate adenocarcinoma patient.

Copyright © 2016, the Authors. Published by Elsevier Inc. under copyright license from the University of Washington. This is an open access article under the CC BY-NC-ND license (<http://creativecommons.org/licenses/by-nc-nd/4.0/>).

## Case report

A 54-year-old man with symptoms of bladder outflow obstruction managed with an alpha blocker, tamsulosin, for 2 months and a 5-alpha reductase inhibitor, finasteride, for 1 month presented to urology clinic with rising prostate-specific antigen (PSA) that was 8.0 ng/mL on referral. He had suffered a coliform urinary tract infection 2 months previously that was managed successfully with antibiotics. Digital rectal examination revealed asymmetric prostate enlargement with a prominent, firm, right prostate lobe. The primary differential diagnosis was prostate adenocarcinoma.

Multiparametric magnetic resonance imaging (mpMRI) was carried out using a 1.5 T system (Signa Excite, GE Healthcare, Little Chalfont, UK) and 8-channel phased array body coil. The MRI protocol included T2-weighted images (T2) in 3 planes, diffusion-weighted imaging (DWI), and dynamic contrast enhanced (DCE) images in the axial plane.

Axial T2 showed homogenous low signal intensity (SI) involving both the peripheral zone (PZ) and transition zone (TZ) and diffusely abutting the capsule (Fig. 1). In addition, evaluation of the right posterolateral PZ at the midland level showed focal obliteration of the capsular signal and infiltration of the periprostatic fat with thickening of the ipsilateral levator ani (Fig. 2). This gave a Prostate Imaging Reporting and

Competing Interests: The authors have declared that no competing interests exist.

\* Corresponding author.

E-mail address: [sumin.lee@southend.nhs.uk](mailto:sumin.lee@southend.nhs.uk) (S.-M. Lee).

<http://dx.doi.org/10.1016/j.radcr.2016.02.009>

1930-0433/Copyright © 2016, the Authors. Published by Elsevier Inc. under copyright license from the University of Washington. This is an open access article under the CC BY-NC-ND license (<http://creativecommons.org/licenses/by-nc-nd/4.0/>).

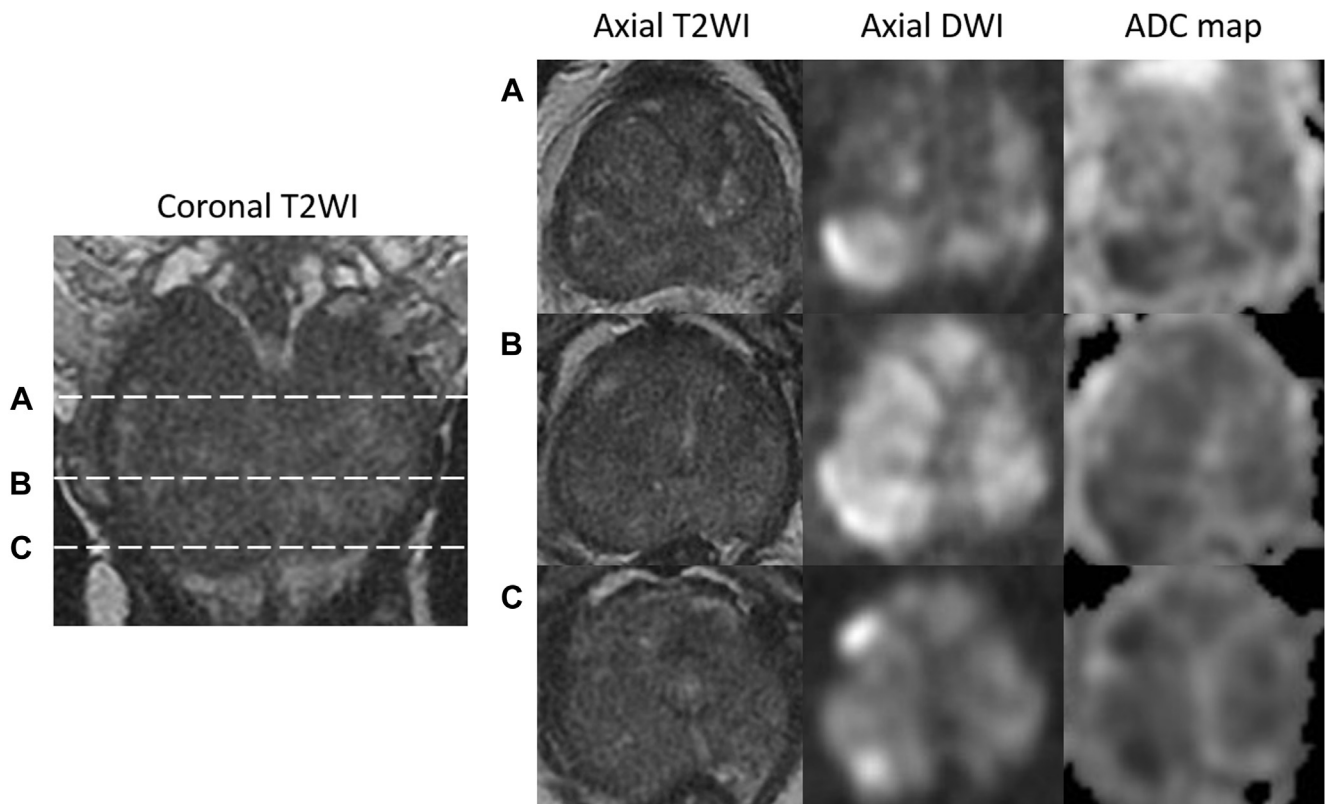


**Fig. 1** – Coronal T2WI and corresponding axial T2WI DWI (b-value 1,400) and ADC maps at the levels of the prostatic base (A), midgland (B), and apex (C), demonstrating diffuse low T2 SI in the PZ and TZ and multifocal areas of high SI on the DWI and low SI on the ADC maps. This results in a PI-RADS v2 score of 5 for both T2WI and DWI [1].

Data System (PI-RADS) v2 score for T2WI of 5 [1]. PI-RADS scoring is summarized in Table 1.

High 1400 b-value DWI revealed high SI throughout the PZ and TZ with multifocal areas of particularly hyperintense SI and corresponding reduced apparent diffusion coefficient (ADC) values, ranging from  $584$  to  $635 \times 10^{-6} \text{ mm}^2/\text{sec}$  (Fig. 3). This resulted in a PI-RADS v2 score for DWI of 5 [1]. DCE color-coded  $k_{\text{trans}}$  images (Fig. 4) showed a type 3 washout curve and asymmetric focal enhancement, scored as “positive” on PI-RADS v2.

As magnetic resonance spectroscopic imaging was not performed, the overall PI-RADS v2 score for the probability of

there being a clinically significant cancer was 5, that is, very high. Thus, a convincing radiologic diagnosis of prostate cancer was made based on the MR images, and the patient was given a provisional stage of T3a N0 disease.

A 42-core, systematic, sector-guided transperineal prostate biopsy, with additional cognitive targeting of the suspicious lesions was performed, as previously described [2,3]. Histologic analysis reported diffuse, nonspecific granulomatous prostatitis (GP). The patient was managed conservatively and discharged from urological care. His lower urinary tract symptoms were well managed on medical therapy.

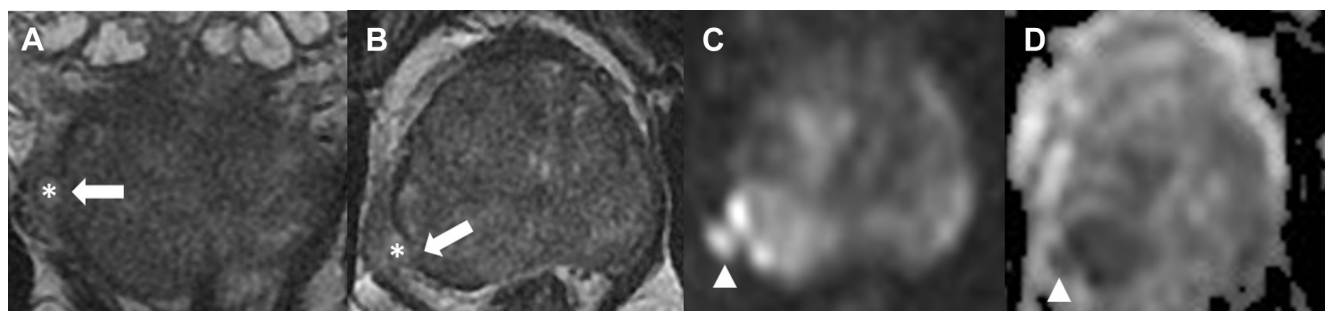


**Fig. 2** – T2WI coronal (A) and axial (B) images showing focal defect in the right posterolateral PZ at the midgland level (white arrows). Abnormal T2 SI (asterisk) extends into the periprostatic fat and demonstrates restricted water diffusion (arrowheads) in the Diffusion Weighted Image (C) and Apparent Diffusion Coefficient map (D). The adjacent levator ani muscle is thickened and of abnormal SI.

**Table 1 – PI-RADS v2 scoring.**

PZ				
DWI score (dominant sequence)	DCE score (secondary sequence)	T2WI score	Overall PI-RADS score	Interpretation
1	Any	Any	1	Significant disease highly unlikely to be present
2	Any	Any	2	Significant disease unlikely to be present
3	–	Any	3	Result equivocal
3	+	Any	4	Significant disease is likely to be present
4	Any	Any	4	Significant disease is likely to be present
5	Any	Any	5	Significant disease is highly likely to be present
TZ				
T2WI score (dominant sequence)	DWI score (secondary sequence)	DCE score	Overall PI-RADS score	Interpretation
1	Any	Any	1	Significant disease highly unlikely to be present
2	Any	Any	2	Significant disease unlikely to be present
3	≤4	Any	3	Result equivocal
3	5	Any	4	Significant disease is likely to be present
4	Any	Any	4	Significant disease is likely to be present
5	Any	Any	5	Significant disease is highly likely to be present

Table adapted from “PI-RADS Prostate Imaging—Reporting and Data System: 2015, version 2” [1]

## Discussion

GP is a heterogeneous condition that describes a granulomatous, inflammatory condition of the prostate. This may be idiopathic, that is, nonspecific, or secondary to causes including specific infections, bacillus Calmette-Guérin (BCG) therapy, surgery, and more rarely, systemic causes [4]. It has an estimated incidence of 3.3% in inflammatory lesions and commonly affects men in their sixth to eighth decades [4].

A popular theory is that nonspecific GP is caused by blockage of the prostatic ducts leading to stasis of secretions and epithelial disruption. Blockage may be secondary to

bacterial products, refluxed urine, or from benign prostatic hyperplasia [4]. Cellular debris and prostatic secretions leak into the stroma, leading to a localized inflammatory response [5]. Infectious GP is most commonly caused by bacteria including tuberculosis and BCG therapy for bladder transitional cell carcinoma or fungi such as blastomycosis or cryptococcosis [5].

This case of nonspecific GP is an example of clinical and radiologic mimicking of prostate adenocarcinoma. Clinically, patients may present with lower urinary tract symptoms including hematuria, urgency, or urinary frequency. The prostate may feel firm or have a hard, fixed nodule on digital rectal examination [4]. Serum PSA levels vary considerably but are raised in a majority of cases.

Radiologically, GP demonstrates tumor-like morphology, with either nodular or diffuse hypoechogenic lesions on ultrasound [6]. The MRI features of BCG-induced GP have been reported to be nonspecific. Naik and Carey [6], who investigated the transrectal ultrasound and MRI (T2- and T1-weighted precontrast and postcontrast) imaging appearances of BCG-induced GP, concluded that there is no pattern of clinical, biochemical, ultrasound, or MRI findings which allow a specific diagnosis of BCG-induced GP to be established or differentiated from prostate cancer. MRI case series for nonspecific GP are limited, with only 2 cases reported by Bour et al [7].

On T2-weighted MRI, GP lesions appear as hypointense SI regions similar to prostate cancer lesions which commonly manifest as round or ill-defined, low SI areas within the PZ [8–10]. Tumors within the TZ are challenging to detect, since the SI of normal TZ and cancer overlap; tumor is often demonstrated as a homogeneous signal mass with blurred margins, the so-called “erased charcoal sign” [8]. High-grade tumors often have reduced SI, as compared with low-grade cancers.

GP and cancer lesions share high SI on DWI at high b-values and low SI on ADC maps [1,8]. ADC values allow

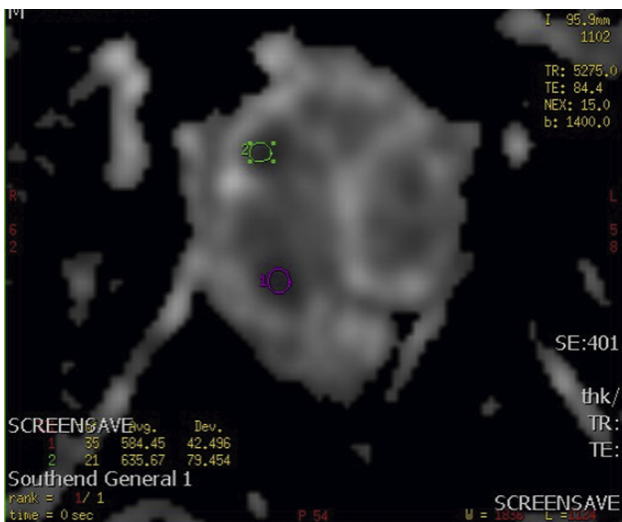


**Fig. 3 – ADC map showing the ADC values ( $10^{-6}$  mm<sup>2</sup>/sec) for 2 regions of interest placed in areas of very low SI on the ADC map (circle 1—ADC value 584 and circle 2—ADC value 635) indicating marked restricted water diffusion.**

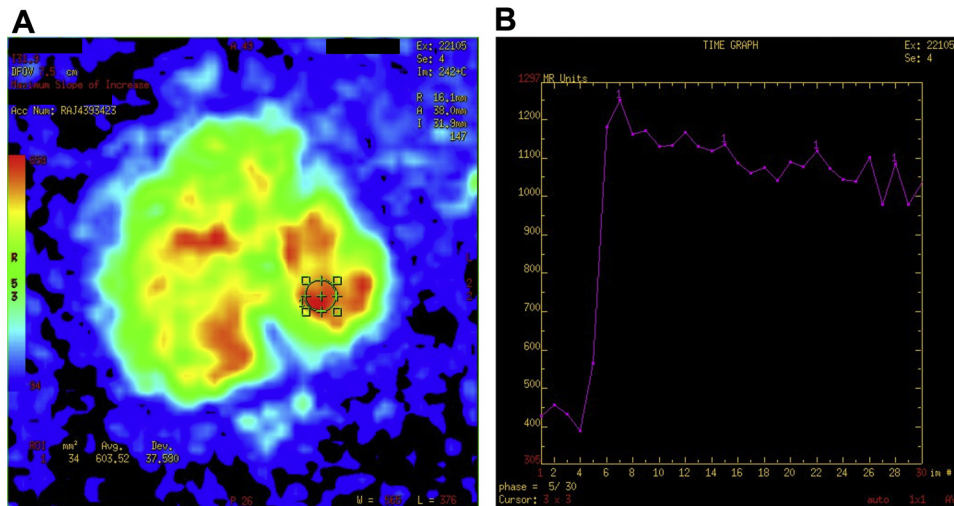


**Fig. 4** – DCE color-coded  $k_{trans}$  image (A) showing asymmetric enhancement (“positive” on PI-RADS v2; 1). Region of interest demonstrates a type 3 (washout) curve (B).

assessment. Lower ADC is associated with cancer and correlate with Gleason scoring [10]. GP demonstrates low ADC values reaching those of the highest Gleason score carcinomas (Fig. 3) [9,10].

Limited studies have investigated the appearances of GP on DCE imaging [7,11]. Bour et al [7] showed only moderate enhancement in cases of non-necrotic granulomatous foci located in the PZ. In contrast, microvessel alterations and neovascularity in prostate cancer cause increased tumor vascularity with early enhancement and rapid washout of contrast material from prostate cancer lesions [1]. Kawada et al [11] showed early and prolonged-ring enhancement in all cases of BCG-induced GP. In our case, the focal area of capsular penetration and extraprostatic spread, in retrospect, shows ring enhancement on the arterial, venous, and equilibrium phases (Fig. 5), consistent with caseous necrosis and small extraprostatic abscess.

Thus, multiparametric MRI appearances simulate prostate cancer [11]. Based on clinical findings and initial investigations, patients often undergo prostate biopsy. In a bid to reduce biopsy morbidity and prevent delays in treatment,

some centers have suggested proceeding directly to radical prostatectomy in patients with high pretest probability of prostate adenocarcinoma [12]; however, a similar policy in this case would have resulted in overtreatment and potentially increased patient morbidity.

Histologically, widespread nonspecific GP may also simulate carcinoma. Typically, nonspecific GP shows a proliferation of epithelioid histiocytes, along with variable numbers of multinucleated giant cells, eosinophils, neutrophils, and lymphocytes (Fig. 6). The epithelioid histiocytes may grow as monomorphic sheets, obliterating normal glandular architecture, and suggesting high grade, that is, Gleason 5, carcinoma [5,13]. Caseation is usually absent in nonspecific GP. Diagnosis may be aided by recognition of the inflammatory nature of cells, along with associated giant cells and fibrosis. Challenging cases may require immunohistochemistry for the identification of epithelioid histiocyte CD68 expression. In contrast, prostate adenocarcinoma expresses PSA, prostate-specific acid phosphatase, and cytokeratins [13].

Infectious causes and postsurgery GP do not usually cause problems in the differential diagnosis. Infectious GP is

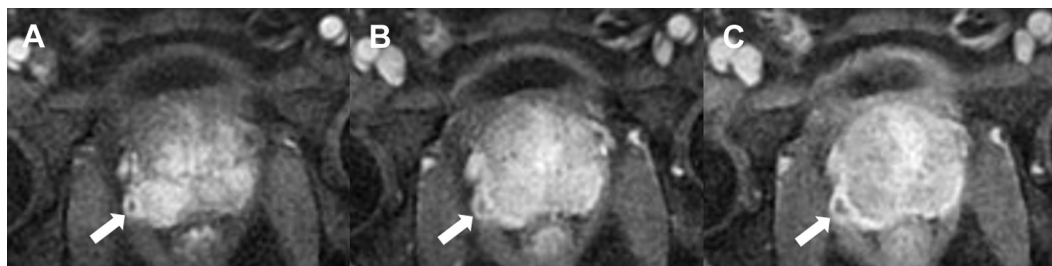


**Fig. 5** – DCE images obtained in arterial (A), venous (B), and equilibrium (C) phases, showing early and prolonged-ring enhancement (arrows) at the site of focal capsular penetration.

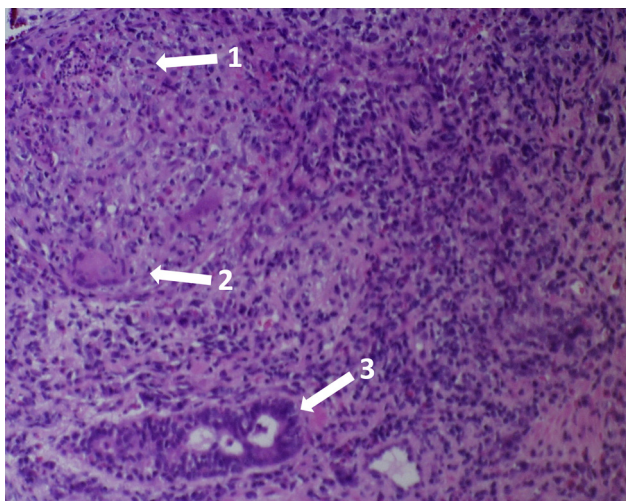


**Fig. 6 – Pathology slide from transperineal biopsy core. Nonspecific GP adjacent to prostatic acinus (3) with a predominant population of mixed inflammatory cell infiltrate including epithelioid histiocytes (1) and giant cells (2).**

usually associated with the presence of multinucleated giant cells and caseation. Patients may have a clinical history of systemic tuberculosis or recent BCG therapy for bladder cancer [14]. Postbiopsy GP patients will have had a recent biopsy or transurethral resection of the prostate; granulomas will be distributed along the surgery and/or biopsy edge on histology [15].

GP is a benign condition. Nonspecific GP resolves naturally through scarring and often needs no further treatment [4]. However, any underlying urinary tract infection should be treated with antibiotic therapy. Patients may continue to be symptomatic during disease resolution and may require supportive measures such as analgesics, in particular nonsteroidal anti-inflammatory drugs [16]. Alpha-receptor antagonists, such as tamsulosin, may help reduce bladder outflow obstruction and improve voiding dysfunction that is common with chronic prostatitis.

## Conclusions

GP is a benign inflammatory condition of the prostate which may be confused clinically, radiologically, and pathologically with prostate adenocarcinoma. Therefore, all patients with suspicious prostate lesions on MRI require formal histopathologic disease confirmation before proceeding to radical treatment.

## REFERENCES

- [1] Weinreb JC, Barentsz JO, Choyke PL, Cornud F, Haider MA, Macura KJ, et al. PI-RADS Prostate Imaging–Reporting and Data System: 2015, Version 2. *Eur Urol* 2016;69(1):16–40.
- [2] Vyas L, Acher P, Kinsella J, Challacombe B, Chang RT, Sturch P, et al. Indications, results and safety profile of transperineal sector biopsies (TPSB) of the prostate: a single centre experience of 634 cases. *BJU Int* 2014;114(1):32–7.
- [3] Kuru TH, Wadhwa K, Chang RT, Echeverria LM, Roethke M, Polson A, et al. Definitions of terms, processes and a minimum dataset for transperineal prostate biopsies: a standardization approach of the Ginsburg Study Group for Enhanced Prostate Diagnostics. *BJU Int* 2013;112(5):568–77.
- [4] Mohan H, Bal A, Punia RP, Bawa AS. Granulomatous prostatitis—an infrequent diagnosis. *Int J Urol* 2005;12(5):474–8.
- [5] Srigley JR. Benign mimickers of prostatic adenocarcinoma. *Mod Pathol* 2004;17(3):328–48.
- [6] Naik KS, Carey BM. The transrectal ultrasound and MRI appearances of granulomatous prostatitis and its differentiation from carcinoma. *Clin Radiol* 1999;54(3):173–5.
- [7] Bour L, Schull A, Delongchamps NB, Beuvon F, Muradyan N, Legmann P, et al. Multiparametric MRI features of granulomatous prostatitis and tubercular prostate abscess. *Diagn Interv Imaging* 2013;94(1):84–90.
- [8] Barentsz JO, Richenberg J, Clements R, Choyke P, Verma S, Villeirs G, et al. ESUR prostate MR guidelines 2012. *Eur Radiol* 2012;22(4):746–57.
- [9] Afaq A, Koh DM, Padhani A, van As N, Sohaib SA. Clinical utility of diffusion-weighted magnetic resonance imaging in prostate cancer. *BJU Int* 2011;108(11):1716–22.
- [10] Turkbey B, Shah VP, Pang Y, Bernardo M, Xu S, Kruecker J, et al. Is apparent diffusion coefficient associated with clinical risk scores for prostate cancers that are visible on 3-T MR images? *Radiology* 2011;258(2):488–95.
- [11] Kawada H, Kanematsu M, Goshima S, Kondo H, Watanabe H, Noda Y, et al. Multiphase contrast-enhanced magnetic resonance imaging features of *Bacillus Calmette-Guerin*-induced granulomatous prostatitis in five patients. *Korean J Radiol* 2015;16(2):342–8.
- [12] Keller A, Kua B. Case report: radical prostatectomy without prostate biopsy in PI-RADS 5 lesions on 3T multi-parametric MRI of the prostate gland. *F1000Research* 2015;54(4).
- [13] Presti B, Weidner N. Granulomatous prostatitis and poorly differentiated prostate carcinoma. Their distinction with the use of immunohistochemical methods. *Am J Clin Pathol* 1991;95(3):330–4.
- [14] Stillwell TJ, Engen DE, Farrow GM. The clinical spectrum of granulomatous prostatitis: a report of 200 cases. *J Urol* 1987;138(2):320–3.
- [15] Eyre RC, Aaronson AG, Weinstein BJ. Palisading granulomas of the prostate associated with prior prostatic surgery. *J Urol* 1986;136(1):121–2.
- [16] Le BV, Schaeffer AJ. Genitourinary pain syndromes, prostatitis, and lower urinary tract symptoms. *Urol Clin North Am* 2009;36(4):527–36. vii.